Mechanics of Advanced Composite Structures

Journal homepage: https://macs.semnan.ac.ir/

Semnan University

ISSN: 2423-7043

Research Article

Tensile, Flexural, and Impact Strength Analysis of a 3D Printed Carbon Fiber Reinforced Nylon Filament

Javed Dhalait[a], Vijay Kumar Jatti[b], Shahid Tamboli[c*], Rakesh Motgi[d]

[a] *Department of Mechanical Engg., A. G. Patil Polytechnic Institute, Solapur, Solapur, 413008, India*
[b] *Department of Mechanical Engineering, Bennett University, 201310, Greater Noida India*
[c] *Department of Mechanical Engineering, Symbiosis Institute of Technology, Symbiosis International University, Pune, 412115, Maharashtra. India*
[d] *Department of Mechanical Engineering, A. G. Patil Polytechnic Institute, Solapur, 413008, Maharashtra. India*

ARTICLE INFO

Article history:

Received:
Revised:
Accepted:

Keywords:

Fused filament fabrication(FFF);
shell count;
infill density;
optimization;
machine learning.

ABSTRACT

3D printing is one of the most popular methods for prototyping and manufacturing lightweight and complex parts in recent years. The fused filament fabrication (FFF) method is preferred due to its ease of operation. Different plastics can be used as additive materials, such as filaments. To enhance the mechanical properties of 3D printed products researchers are developing new composite materials. By varying the parameters associated with the manufacturing of these materials, mechanical properties can be altered. This study aimed to find out the effect of printing parameters in Carbon fiber-reinforced Nylon to get better mechanical properties. In this study chopped carbon fibers are reinforced in Nylon base material to get the 'FFF 3D printing' filament material. Infill density and shell perimeter were varied to get different specimen types. The specimens were prepared as per the ASTM standards for the tensile, flexural, and impact testing. Machine learning is used to predict the parameters for tensile, flexural, and impact strength. The study shows the effect of printing parameters on mechanical properties like flexural strength and tensile strength. Infill percentage shows a significant effect on mechanical strength. The ML regression model shows higher accuracy for tensile strength than the flexural and impact strength.

1. Introduction

3D printing is also known as rapid prototyping. It is popular for producing prototypes at a fast speed and with low wastage. Different types of 3D printing are selective stereolithography (SLA), selective laser melting (SLM), fused filament fabrication (FFF) or material extrusion (MEX), and laminated body manufacturing (LBM) [1]. The plastic filament of small diameter is fed to the nozzle and the object is built layer by layer [2,3]. This ease in FFF is popular among industry and researchers. The lightweight part is easy to post-process [4-6]. The deposition of layers and forming of the part is carried out with the help of slicing software. In the slicing process, various parameters are selected. Studies are carried out to see the effect of infill percentage, infill pattern, shell thickness, raster angle, printing temperature, and printing speed[7,8]. Different studies have been carried out to optimize different parameters for 3D printing. 'Desing of Experiments, DoEs' have been set up to get the results [9].

The polymers used in 3D printing need to be optimized for suitable industrial use. The need

* **Corresponding author.**
E-mail address: *shahidt@sitpune.edu.in*

Cite this article as:
Javed Dhalait, Vijay Kumar Jatti, Shahid Tamboli, Rakesh Motgi, 2025. Tensile, Flexural and Impact Strength Analysis of a 3D Printed Carbon Fiber Reinforced Nylon Filament. *Mechanics of Advanced Composite Structures*, 12(1), pp. xx-xx
https://doi.org/10.22075/MACS.2024.39315.2050

for better working properties led to the use of composite filament[10-12]. The flexibility of the process is that the user can use different materials in different filament forms. Researchers have tried to improve properties by adding natural fibers, synthetic fibers, metallic particles, wooden particles, and natural particles to get better results. In natural fibers, coconut husk, bamboo, hemp, and rice straw fibers are used in the composite material. Natural fibers have limitations in use [13]. To overcome these limitations synthetic fibers like glass, Kevlar, Graphene, and Carbon fiber are used [14,15]. Carbon fiber is the most preferred material by researchers. Carbon fibers are used with different base materials like PLA, Nylon, PETG, and ABS [16,17]. In one of the studies for biomedical and aerospace applications, layer thickness was found to play a key role in determining material strength. This study found that thinner layers (0.1 mm) and higher infill densities improve the tensile, flexural, and impact strengths of polyamide samples due to better bonding and fewer air voids [18]. The degradation of mechanical properties in the composite material exposed to sunlight was studied with reference to the infill density and layer thickness. FTIR analysis and scanning electron microscopy (SEM) revealed the surface degradation, the internal structure remained stable, primarily influenced by infill density and layer thickness [19]. Carbon fibers are used in two methods. It can be extruded by a nozzle on plastic, or it can be embedded in the filaments [20,21]. Digamba Bilkar et al. [22]developed a filament by adding Carbon nanofiber to the ABS filament and tested the mechanical properties. Improved mechanical properties were found in this study. Dilip S. Choudhari et al [23] added chopped Carbon fiber to Nylon 66 in different weight percentages. Better mechanical properties were observed for an increased percentage of Carbon fiber. Common printing errors like nozzle jams and layer misalignments remain a challenge in Fused Filament Fabrication (FFF), leading to material and time waste. Zhang et al. introduced a deep learning (DL)--based method to monitor and detect printing failures in real-time, achieving high accuracy in beta tests on a commercial FFF setup [24]. In a one-of-a-kind review, Nishata Royan et al. [25] summarized the advantages and limitations of natural fiber. It also highlighted that the use of natural fiber composite led to the betterment of properties. Ibrahim M. Alarifi [26] evaluated the performance of the 3D-printed combination of nylon and glass fiber. He considered different raster orientations and performed flexural tests. Improved flexural strength was observed in his study. Ismail Fidan et al. [27] studied the current trends in fiber-reinforced additive manufacturing (FRAM). They highlighted the effect of different fibers used and their effect on the mechanical properties. The study also pointed out the application of FRAM in the current scenario. Mahdi Mohammadizadeh et Al. [28] found out that the orientation of carbon fiber has a substantial effect on mechanical properties. Orkhan Huseynov et al. [29] studied the effect of the matrix on the thermal properties of the composite materials. Mishra et. al. [30] examined the low-energy impact resistance of 3D-printed thermoplastic and thermoset carbon fiber composites, focusing on infill density effects through Izod impact testing. Heat treatment effects were also evaluated, with fracture surfaces analyzed by scanning electron microscopy. It was found that infill density and fiber type strongly affect the impact resistance, with coextruded fiber composites at 75% infill achieving the highest impact resistance.

It was felt that instead of testing the 3D printed part for one particular type of loading; impact, tensile, and flexural testing need to be carried out in a single study. It was concluded that a machine learning approach is necessary to predict the 3D printing parameters. Hence as a novel approach, machine learning was applied to find the optimal 3D printing parameters for improving the mechanical properties of Carbon fiber-reinforced nylon. The following tasks were identified and accomplished in this study.

1. Selection of the material - Carbon fibers were chopped and reinforced into a Nylon base to create the filament material for FFF 3D printing.
2. To vary infill density and shell perimeter to produce different specimen types.
3. To prepare the samples in accordance with ASTM standards for tensile, flexural, and impact testing.
4. Apply a machine learning regression model to predict the effect of printing parameters to enhance the tensile, flexural, and impact strength.

2. Material and Methodology

2.1. Methodology

Based on the literature review 3D printing parameters were selected with the help of literature reviews. External shell perimeter and infill percentage affect the mechanical properties of the 3D printed part. Three levels were selected as low, medium, and high for *the* Taguchi L9 array. The external shell count 2 was selected as low and 6 as high level. Infill density was varied from 20 to 60 percent. Table 1 shows three different levels selected for the specimen preparation.

Table 1. Design of experiment

Level	Parameters	
	External Shell Count	Infill Density
Level I (Low)	2	20
Level II (Medium)	4	40
Level III (High)	6	60

2.2 Material

The filament was provided by Anisoprint. It was manufactured by adding chopped Carbon fiber to the Nylon polymer material. Chopped Carbon fiber with 1.75 mm diameter was used for this addition.

2.3 3D Printer

Composer A4, a 3D printer manufactured by Anisoprint was used for this study. This is one of the desktop 3D printers, that works on composite fiber co-extrusion as well as FFF technology. This printer uses Aura II as slicing software. The nozzle (hardened) diameter was 0.4 mm. This printer has a layer resolution of up to 100 microns. Figure 1 shows the Anisoprint Composer A4, a 3D printer used for manufacturing the specimen whereas Table 2 has the key parameters used in the 3D printing of the specimen.

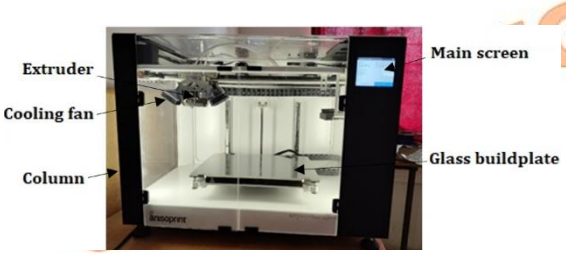

Fig. 1. Anisoprint Composer A4, 3D printer

Table 2. A key parameter in 3D printing

Sr. No.	Parameter	Value Set
1	Printing temperature	250°
2	Build plate temperature	40°
3	Infill pattern	Anisogrid
4	Top and bottom layer count	2
5	Layer height	0.2 mm

2.4 External Shell Count

The shell perimeter in 3D printing refers to the outer walls or layers that form the external boundary of the printed object. It represents the number of solid layers or "shells" that are printed around the infill structure. A thicker shell (with more perimeter layers) increases the strength, durability, and surface quality of the object, as it provides a more robust outer structure, protecting the internal infill. The shell perimeter is typically set in terms of the number of layers or wall thickness, and adjusting it influences the mechanical properties and print quality of the final part. Three levels of shell perimeters selected for this study are mentioned below.

Shell count 2 was assigned as low level as it is the basic level required to form a rigid body whereas 4 was assigned to a medium level. 6 was assigned as high level as the increase in shell thickness increases material requirement and deposition time.

2.5 Infill Density

Infill density in a 3D-printed part refers to the amount of material used to fill the interior of the object. It is expressed as a percentage, where 0% represents a completely hollow object, and 100% indicates a fully solid part. The infill density affects the part's weight, strength, and material usage. Higher infill densities increase the strength and rigidity of the printed object but use more material and require longer printing time. Lower infill densities make the object lighter and quicker to print but reduce its structural integrity. Three levels of densities were selected 20%, 40%, and 60%. 20% is considered a low level, as it provides sufficient infill strength against compression required to form a rigid body. 60% is considered a high level because the increase in infill percentage beyond 60% will decrease the air gap inside the body, resulting in a nearly solid body.

2.6 Sample Preparation

Specimens were prepared as per the ASTM D standards. The following subsection discusses the details of the three different tests.

2.6.1Izod Impact Test

The impact test specimen is a small, notched sample. The notch is a critical feature as it creates a localized stress concentration, which influences how the material will fracture under the impact. The absorbed impact energy is recorded in Joules and indicates the material's ability to resist the impact forces. Higher energy absorption indicates better impact resistance. Figure 2a shows the Izod impact test specimen prepared as per the ASTM D 256 standard [31] whereas Figure 2b shows the Izod impact test setup.

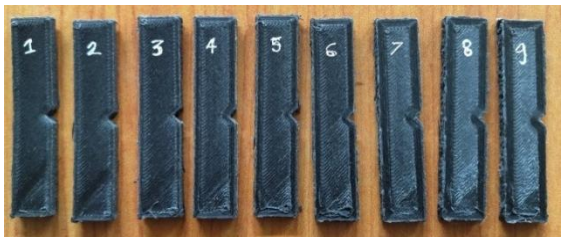

Fig 2a. Izod impact test specimen (Notched) ASTM D256 standard

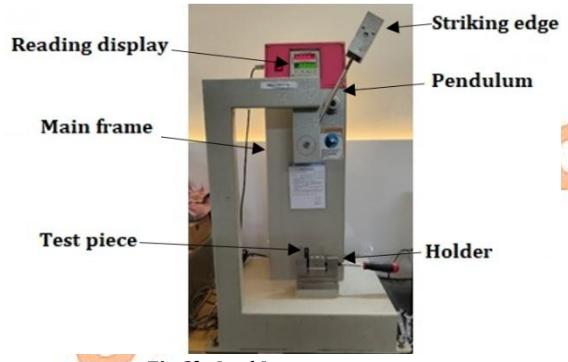

Fig 2b. Izod Impact test setup

2.6.2 Flexural Test

The ASTM D 790 standard [32] Specifies the procedure for conducting a flexural test. Unlike impact tests, the flexural test specimens typically do not require notches. The focus is on measuring bending strength and modulus without introducing stress concentrations. The span between the supports should be 16 times the thickness of the specimen. This ensures that the bending stress is distributed properly across the specimen. The flexural strength is calculated based on the maximum load the specimen can withstand before the failure. The standard formula involves the applied load, span length, and specimen dimensions. Figure 3a shows the specimen prepared as per the ASTM D790 standards whereas Figure 3b shows the flexural test setup.

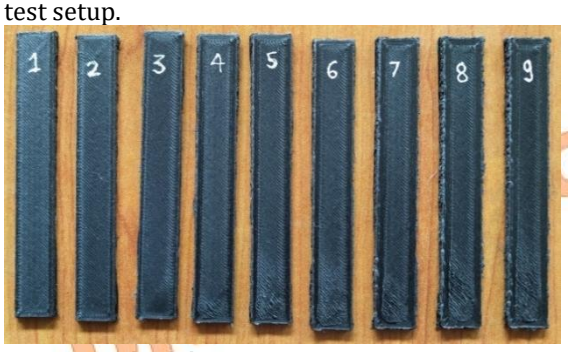

Fig 3a. Flexural-test-specimen-as-per-ASTM-D790

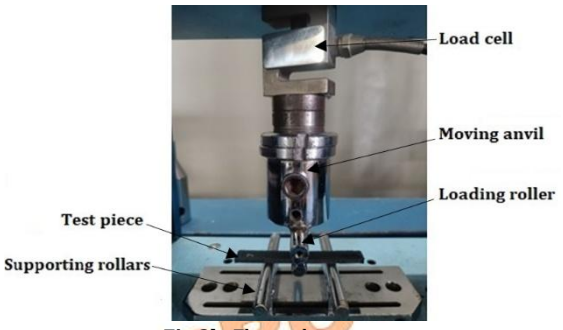

Fig 3b. Flexural test setup

2.6.3 Tensile Test

ASTM D 638 [33] is the standard for testing the tensile properties of a plastic material. Specimens were clamped in a tensile testing machine using grips designed to hold the specimen securely without introducing additional stress or deformation. Figure 4a shows the specimen prepared for the tensile test whereas Figure 4b shows the tensile test experiment setup.

Fig 4a. Tensile strength sample ASTM D 638 standard

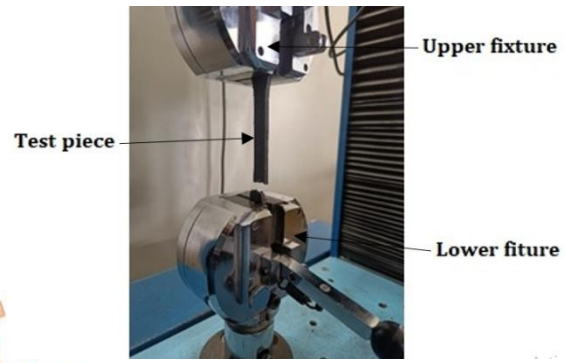

Fig. 4b. Tensile test setup

2.7 Taguchi method

The Taguchi method was employed in this study to enhance the quality of the process by using carefully designed experiments. It involves:

• Design of Experiments (DOE): Selecting factors and levels to test.

• Orthogonal Arrays (OAs): Utilizing predefined arrays like L4, L8, L9, L27, etc., to efficiently assess the impact of various factors while reducing the number of required experiments.

• Analysis: Evaluating results through the calculation of S/N ratios and mean values to identify optimal conditions.

In Taguchi's experimental design, the procedure involves the use of orthogonal arrays of various levels to optimize design parameters (controllable factors) and noise factors (uncontrollable factors). For this study, a three-factor, three-level setup was selected.

2.7.1 Signal-to-Noise (S/N) Ratio

In Taguchi's approach, the S/N ratio is a crucial metric for assessing the robustness of the process or product:

• Higher is Better: For characteristics where larger values are preferable, the S/N ratio is calculated to quantify performance stability. In this regard, the S/N ratio is calculated from equation no. 1

$$S/N = -10*\log(\Sigma(1/Y^2)/n) \quad (1)$$

where 'Y' is responses for the given factor level combination and 'n' is the number of responses in the factor level combination.

• Lower is Better: For characteristics where smaller values are desired, the S/N ratio reflects the reduction in undesired outcomes. S/N value is calculated from equation no. 2

$$S/N = -10*\log(\Sigma(Y^2)/n) \quad (2)$$

Where 'Y' is responses for the given factor level combination and 'n' is the number of responses in the factor level combination.

• Nominal is Better: For characteristics aimed at a specific target value, the S/N ratio measures how closely the results approach the desired nominal value. For this S/N value is calculated from equation no. 3

$$S/N = -10*\log(s^2) \quad (3)$$

where 's' is the standard deviation of the responses for all noise factors for the given factor level combination.

The S/N ratio considers both the mean performance and the variability. It provides an indication of how consistently the desired outcomes are achieved.

2.7.2 Mean vs. Control Factors

When analyzing experimental results, both mean values and S/N ratios are considered.

Mean Values: Represent the average performance under different experimental conditions. These values are used to determine which settings produce the best average outcome.

S/N Ratios: Reflect the robustness of the process or product, indicating how stable the performance is; with respect to the variability. Higher S/N ratios are preferred as they denote better performance consistency.

2.8 Machine Learning in MATLAB

Machine learning has become increasingly important in modern times, and the use of AI is proving to be highly beneficial in the field of engineering. As a subset of AI, machine learning enables systems to receive input data and generate corresponding outputs. Through various algorithms and datasets, machines can learn and improve their performance over time. In MATLAB, regression models serve as powerful tools for analyzing and predicting relationships between variables. The R-squared value plays a key role in assessing the quality of these models, as it indicates how well the independent variables account for the variance in the dependent variable. The results obtained are used to predict values by utilizing the regression learner in MATLAB.

The result and discussion section compiles all the data from the experiment. It also discusses analysis performed on the data through the Taguchi method as well as through machine learning.

3. Figures and Tables

3.1 Results from the Experiments

Results conducted on impact, tensile as well as flexural setup are mentioned in Table 3.

Table 3. Result for Izod Impact, Tensile, and flexural tests

Sample. No.	Impact Value (J/m)	Tensile Strength (MPa)	Flexural Strength (MPa)
1	100	11.31	30.35
2	100	15.11	33.33
3	109.5	18.27	34.52
4	95.2	15.22	31.54
5	119.5	16.70	37.50
6	133.3	19.95	36.30
7	104.7	16.01	35.71
8	109.5	17.73	36.90
9	138.0	20.97	36.30

3.1.1 Impact Test Results

Impact value is a measure of the material's toughness, indicating the amount of energy it can absorb before fracturing. From the above table, we can say that the impact strength value ranges from 100 J/m to 138 J/m. The impact values increase from sample 1 to sample 9. It has one exception of 95.2 J/m. This implies that sample 9 can absorb more energy and may be tougher compared to the others.

3.1.2 Tensile Test Results

Tensile strength is the maximum stress that a material can withstand while being stretched or pulled before breaking. It ranges from 11.31 MPa to 20.97 MPa. The tensile strength increases as well as the impact value increases, with sample 9 having the highest tensile strength. Sample 1 has the lowest tensile strength and impact value, indicating it might be more brittle. Samples with higher impact values exhibit higher tensile strengths, suggesting a correlation between toughness and tensile strength.

3.1.3 Flexural Strength Results

Flexural strength measures a material's ability to resist deformation under the load. In this work, it ranges from 30.35 MPa to 37.50 MPa. Flexural strength shows less variation compared to tensile strength. The values are quite close, ranging between 30.35 MPa and 37.50 MPa. It suggests that the material's ability to resist bending does not change drastically across the samples, though sample 5 stands out with the highest flexural strength.

Overall performance of sample 9 seems to be the best-performing in terms of toughness and tensile strength, while sample 5 performs best in terms of flexural strength. Sample 1, on the other hand, shows the lowest performance in both impact and tensile strength.

Results mentioned above were analyzed by two methods 1) Taguchi design in MINITAB and 2) Machine learning in MATLAB.

3.2.1 Result Analysis of Impact Strength

The results of the Impact Test were put into Minitab software's Taguchi L9 array and the following output was obtained. Table 4 indicates the response table for means for impact strength wherein larger is better. Whereas Table 5 shows the signal-to-noise ratio.

Table 4. Response Table for Means

Level	Shell count	Infill density
1	0.4333	0.4200
2	0.4867	0.4600
3	0.4933	0.5333
Delta	0.0600	0.1133
Rank	2	1

As the infill percentage increases the response value increases from level 1 to level 3. This indicates that infill percentage has a positive effect on manufactured products. Delta represents the range of variation in the response due to changes in the shell count. The comparatively small delta indicates that shell count has a small influence. Shell count is less significant compared to infill density. An increase in shell count shows the response values increase as the infill density increases.

Table 5. Response Table for Signal-to-Noise Rations (Larger is better)

Level	Shell count	Infill density
1	-7.272	-7.542
2	-6.339	-6.767
3	-6.202	-5.504
Delta	1.069	2.037
Rank	2	1

The response value increases as the infill density goes from Level 1 to Level 3. This indicates that increasing the infill density has a positive effect on the outcome, suggesting that higher infill density leads to stronger or more durable structures. The relatively small delta suggests that while shell count influences the outcome, its effect is less significant compared to infill density. Shell count is the second most influential factor in this experiment.

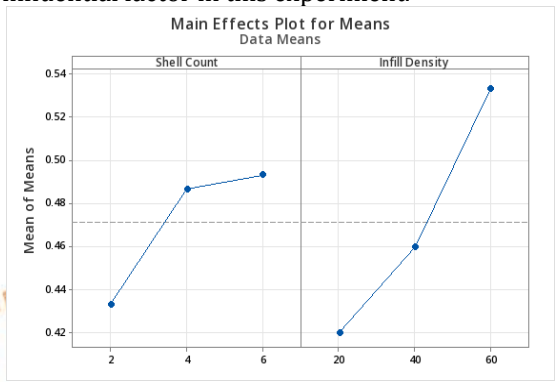

Fig 5. Main effects plot for means for impact test

The key impact plot for methods frequently employed in the design of experimentation (DOE) is shown in Figure 5. It is beneficial to comprehend how various factors influence a process or system's mean response. A greater impact on the reaction is indicated by an increase in the slope. A discernible rise in the mean reaction occurs when the shell count is increased from two to four. There is just a small improvement when it is increased from 4 to 6, indicating that the benefits decrease as the number of shells grows. Compared to shell count,

infill density has a more noticeable impact. There is a sharp increase in the average reply when the infill density is increased from 20 to 40.

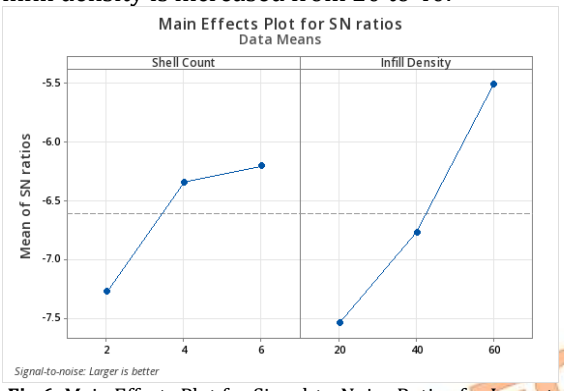

Fig 6. Main Effects Plot for Signal-to-Noise Ratios for Impact Test

Figure 6 is a main effects plot for SN ratios (Signal-to-Noise Ratios), which is often used in robust design and Taguchi methods for quality improvement. The purpose of this plot is to show the effects of different factor levels on the signal-to-noise (S/N) ratio, where higher values typically indicate better performance. The S/N ratio increases significantly from shell count 2 to 4. There is a slight increase from shell count 4 to 6, indicating a diminishing return on increasing the shell count. The S/N ratio sharply increases as the infill density increases from 20 to 60, which suggests that higher infill density positively affects the signal-to-noise ratio. Increasing infill density has a more pronounced positive effect on the s/n ratio than shell count, as shown by the steeper slope in the second panel. Shell count shows improvement, but the effect diminishes after reaching a certain point.

3.2.2 Result Analysis of Tensile Strength

Table 6 shows that the response value rises with each level of infill density, indicating that the performance parameter gets better as the infill density rises. At Level 3, the greatest reaction is observed. The response value increases with the increase in infill density. This suggests that improved performance is achieved by a higher infill density. The values range from 19.73 to 14.18, showing a difference larger than the shell count delta.

Table 6. Response Table for Means (Larger Is Better)

Level	Shell count	Infill density
1	14.90	14.18
2	17.29	16.51
3	18.24	19.73
Delta	3.34	5.55
Rank	2	1

As the shell count increases from Level 1 to Level 3, Table 7 displays an increase in response values, indicating that a greater shell count has a beneficial impact on the result. A comparatively decreasing delta indicates that the shell count has a moderate impact on the result. Greater infill densities are correlated with greater response values, indicating that more infill shows better results. At Level 3, a significant response is observed.

Table 7. Response Table for Signal-to-Noise Rations (Larger is better)

Level	Shell count	Infill density
1	23.30	22.94
2	24.70	24.34
3	25.16	25.89
Delta	1.87	2.95
Rank	2	1

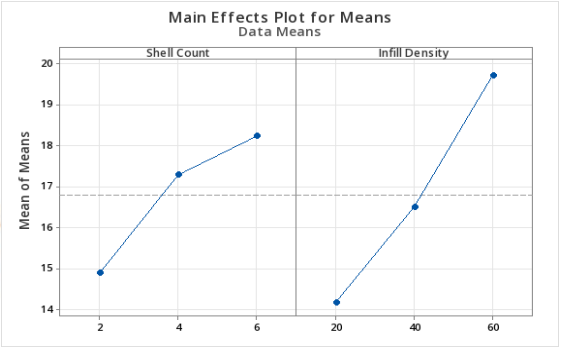

Fig 7. Main Effects Plot for Means for Tensile Test

Figure 7 indicates that the response variable is positively affected by the infill density and the shell count. The effect of infill density seems to be greater compared to that of the shell count, especially when the infill density rises from 40 to 60. Increasing these parameters (such as infill density) can result in greater efficiency in the response to the variable under consideration.

Figure 8 demonstrates that the SN ratio is benefited by both shell count and infill density, indicating that increasing both parameters increases the quality or performance. The effect of infill density becomes more apparent and steadier, especially at higher densities (40 and 60).

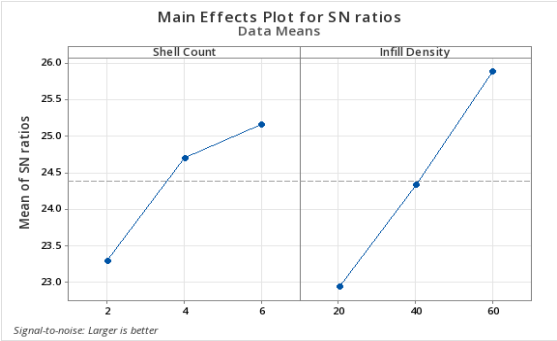

Fig 8. Main Effects Plot for Signal-to-Noise Ratios for Tensile Test

This shows that improving infill density than shell count is giving more significant gains in quality or strength. Shell count has a saturation effect after four shells, which means that more shell count will not improve the results.

3.2.3 Result Analysis of Flexural Strength

As shown in Table 8, as the shell count increases from Level 1 to Level 3, the outcome improves. The outcome improves as infill density increases, but the highest performance is observed at Level 2 with a value reading of 35.91, whereas Level 3's value is recorded as slightly lower at 35.71. The variation between level 1 and level 2 is very small, this shows that infill density has a slightly smaller effect compared to the shell count. Infill density is ranked as the second factor, indicating it has a smaller impact than the shell count.

Table 8. Response Table for Means (Larger Is Better)

Level	Shell count	Infill density
1	32.73	32.53
2	35.11	35.91
3	36.30	35.71
Delta	3.57	3.38
Rank	1	2

From Table 9, we can observe that performance outcome improves as the shell count increases from Level 1 to Level 3, but the changes are relatively small. The highest outcome is at Level 3 value of 31.20, indicating that a higher shell count does lead to improved performance. This is indicated by a delta 0.91 which is the difference between the highest 31.20 and lowest 30.29 values. The small delta shows that infill density has no significant effect on the outcome. Its significance is slightly less than the shell count. Infill density is ranked as the second most influential factor.

In Figure 9, we can see that shell count has a strong positive effect on the response, with no indication of diminishing returns in the observed range. A higher shell count directly leads to an improved outcome.

Table 9. Response Table for Signal-to-Noise Rations (Larger is better)

Level	Shell count	Infill density
1	30.29	30.23
2	30.89	31.09
3	31.20	31.05
Delta	0.91	0.87
Rank	1	2

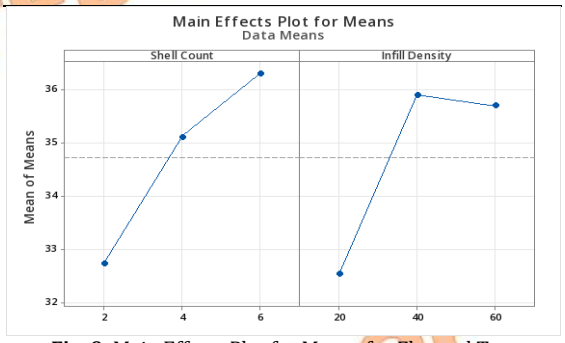

Fig. 9. Main Effects Plot for Means for Flexural Test

Infill density also affects the response, but there appears to be an optimal level at 40. Increasing the infill density after 40 can cause a small decline in strength. This may cause an increase in infill density, leading to a change in physical properties.

Fig. 10. Main Effects Plot for Signal-to-Noise Ratios for Flexural Test

The increase in shell count shows an increase in mechanical properties. An increase in infill density after a point shows a decline in flexural strength. This point needs further attention. From Taguchi analysis, it is observed that a higher shell count shows better output. However, in some cases, it is observed that after shell count 4, there is no significant rise in mechanical properties. That means the shell count should be moderate; increasing the shell count largely will not give better results. Elevated infill density shows better results. It is observed that in the case of tensile and impact tests, density at 60% shows better accuracy than 40% density. However, in the flexural test, the increase in infill density shows a decrease in mechanical strength. This indicates that after 40% infill density

flexural strength does not improve significantly. Further study is needed to find out what is the reason for this decrease and what percentage of drop in flexural strength is observed.

3.3 Result Analysis by Machine Learning Approach

Regression models in MATLAB provide powerful tools for analyzing and predicting relationships between variables [34]. The R-squared value is a crucial metric for evaluating the goodness of fit of these models, to understand how well the independent variables explain the variability of the dependent variable [35,36]. The results obtained are used for determining the predicted values using regression learning in MATLAB. Table 10 represents the evaluation metrics for a trained Linear Regression model for the tensile test.

Table 10. ML Models for Tensile Test Training Results

RMSE (Validation)	0.93977
R-Squared (Validation)	0.92
MSE (Validation)	0.88317
MAE (Validation)	0.73846
MAPE (Validation)	5.0%

Table 10 shows how the model, with an R-squared value of 0.92, or 92%, can account for the variance of the target variable. It indicates that the data fits well. The model with low levels of error metrics such as RMSE (0.93977), MSE (0.88317), and MAE (0.73846) shows that the model's predictions are near to actual data. The predictions by the model deviate 5% from the true values. The mean absolute percentage error (MAPE) of 5.0%, is acceptable.

In Table 11, the R-squared value is 0.67, showing that the model explains 67% of the variance in the target variable. This indicates a moderate fit. This model shows a higher error compared with other models. The values RMSE (1.6087), MSE (2.5881), and MAE (1.4034) indicate that the predictions have less preciseness. The model's average deviation from true values is 4.1%, as indicated by the comparatively low degree MAPE of 4.1%. There are numerous real-world situations when this 10% mistake is acceptable. With comparatively higher error rates and reasonable accuracy (R-squared = 0.67), this linear regression model shows potential for improvement in prediction ability. Though not very accurate, the model's small size and low MAPE (4.1%) make it a good choice in situations where speed and resource efficiency are important.

The R-squared value of 0.65 in Table 12 means that 65% of the variation in the variable of interest, can be explained by the model. This

Table 11. ML Models for Flexural Test Training Results

RMSE (Validation)	1.6087
R-Squared (Validation)	0.67
MSE (Validation)	2.5881
MAE (Validation)	1.4034
MAPE (Validation)	4.1%

Indicates a mediocre fit, which means that the model may not account for all the factors influencing the target variable. Relatively small prediction mistakes are indicated by error metrics. These modest RMSE (0.040514), MSE (0.0016414), and MAE (0.035516) values indicate that the model performed reasonably well, with predictions that are close to the actual values. The model's predictions differ from the true values by an average of 7.7%, as shown by the MAPE of 7.7%. Even though this is a little higher, the scenario and the application area still make it appropriate.

Table 12. ML Models for Impact Test Training Results

RMSE (Validation)	0.040514
R-Squared (Validation)	0.65
MSE (Validation)	0.0016414
MAE (Validation)	0.035516
MAPE (Validation)	7.7%

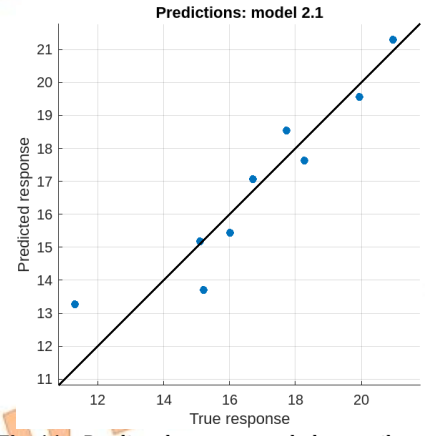

Fig. 11a. Predicted versus actual plot tensile test

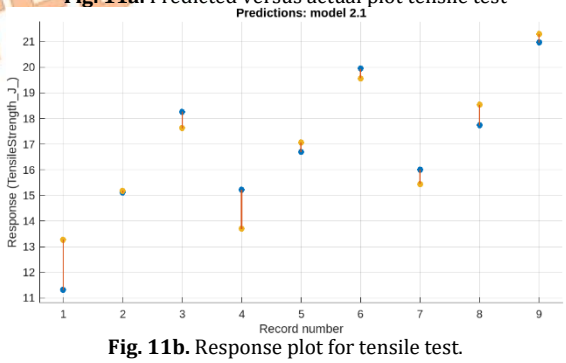

Fig. 11b. Response plot for tensile test.

A scatter plot comparing the true (x-axis) and expected (y-axis) responses is shown in Figure 11(a). It displays the line of perfect prediction, where values that are anticipated coincide with actual values exactly. A point completely aligns

the model's predicted value with the actual value if it falls on this line. Every dot shows the difference between the model's forecast and the actual value. The accuracy of the model increases with the distance between these spots and the black line. There is some variance, most of the locations are quite close to the diagonal line, suggesting that the model is reasonably accurate. However, there is some deviation. The spread of the points indicates that while predictions are generally good, there may be some degree of under-prediction (where points fall below the line) and over-prediction (where points fall above the line). Improving the model to handle these cases in a better way will improve its overall accuracy. Further statistical metrics, such as RMSE or R-squared, would help quantify the exact performance.

Figure 11 (b) is a response plot of the data points which are numbered from 1 to 9, representing different observations or records. The Y-axis (Response – Tensile Strength) represents the response variable as a tensile strength. The difference between the actual and projected figures can be seen by the vertical lines joining the orange and blue dots. The error, or discrepancy, between the actual value and the model's projected one, increases with the length of the line. The projected values for a number of records (records 5 and 9) are extremely close to the true values, suggesting that the model performs well in terms of prediction for those data points. The longer vertical error bars for records 1 and 7 suggest that there are more substantial differences between the true and anticipated values.

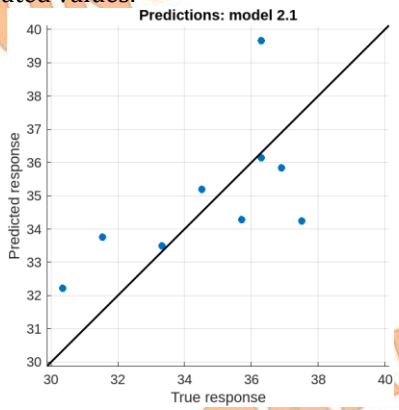

Fig. 12a. Predicted versus actual plot flexural test

The plots for flexural and impact tests (Figure 12 and Figure 13) show the models have less accuracy compared to the models for tensile strength. It also shows more errors. This needs further attention.

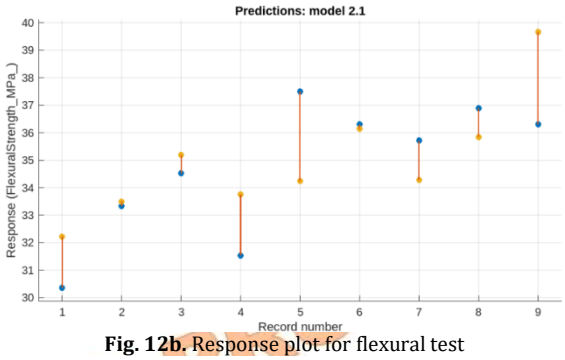

Fig. 12b. Response plot for flexural test

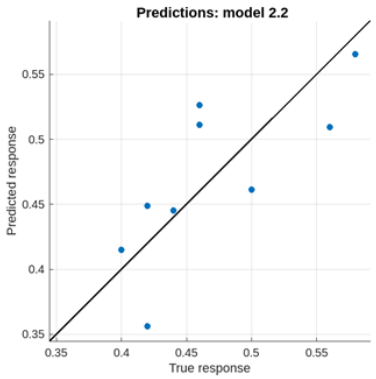

Fig. 13a. Predicted versus actual plot impact test

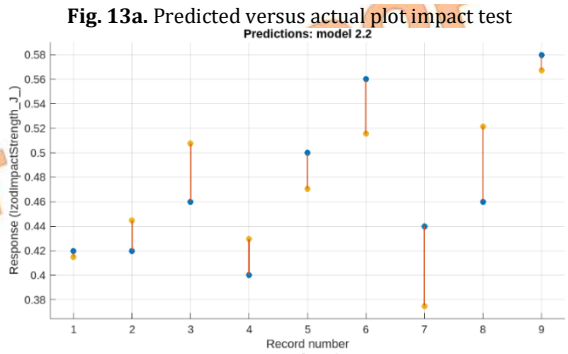

Fig. 13a. Response plot for impact test

Conclusion

The study investigated the effects of infill density and shell count in FDM 3D printing on the mechanical properties of Carbon fiber-reinforced nylon specimens. Optimal combinations were found to be 60% infill density with 6 shells, which yielded the highest impact and tensile strength, while maximum infill with 4 shells provided the best flexural strength. Sample 9 excelled in tensile strength and impact resistance, suitable for tough applications, while Sample 5 had superior flexural strength for bending resistance. Analysis showed infill density as the dominant factor. Regression modeling yielded high accuracy for tensile strength but moderate accuracy for flexural and impact strength, indicating further study is needed. The use of different parameters and an increase in the number of samples can be done in the future.

Funding Statement

This research did not receive any specific grant from funding agencies in the public, commercial, or not-for-profit sectors.

Conflicts of Interest

The author declares that there is no conflict of interest regarding the publication of this article.

References

[1] Ismail, K.I., Yap, T.C. and Ahmed, R. (2022). 3D-Printed Fiber-Reinforced Polymer Composites by Fused Deposition Modelling (FDM): Fiber Length and Fiber Implementation Techniques. Polymers, 14(21),p.4659. doi:https://doi.org/10.3390/polym14214659..

[2] Bochnia, J., Blasiak, M. and Kozior, T. (2021). A Comparative Study of the Mechanical Properties of FDM 3D Prints Made of PLA and Carbon Fiber-Reinforced PLA for Thin-Walled Applications. Materials, 14(22), p.7062. doi:https://doi.org/10.3390/ma14227062..

[3] Chaudhry, F.N., Butt, S.I., Mubashar, A., Naveed, A.B., Imran, S.H. and Faping, Z. (2019). Effect of carbon fibre on reinforcement of thermoplastics using FDM and RSM. Journal of Thermoplastic Composite Materials, 35(3), pp.352–374. doi:https://doi.org/10.1177/0892705719886891.

[4] Akhoundi, B., Behravesh, A.H. and Bagheri Saed, A. (2018). Improving mechanical properties of continuous fiber-reinforced thermoplastic composites produced by FDM 3D printer. Journal of Reinforced Plastics and Composites, [online] 38(3), pp.99–116. doi:https://doi.org/10.1177/0731684418807300.

[5] Guduru, K.K. and Srinivasu, G. (2020). Effect of post treatment on tensile properties of carbon reinforced PLA composite by 3D printing. Materials Today: Proceedings. doi:https://doi.org/10.1016/j.matpr.2020.03.128.

[6] Maqsood, N. and Rimašauskas, M. (2021). Delamination observation occurred during the flexural bending in additively manufactured PLA-short carbon fiber filament reinforced with continuous carbon fiber composite. Results in Engineering, 11, p.100246. doi:https://doi.org/10.1016/j.rineng.2021.100246.

[7] Heidari-Rarani, M., Rafiee-Afarani, M. and Zahedi, A.M. (2019). Mechanical characterization of FDM 3D printing of continuous carbon fiber reinforced PLA composites. Composites Part B: Engineering, [online] 175, p.107147. doi:https://doi.org/10.1016/j.compositesb.2019.107147.

[8] de Toro, E.V., Sobrino, J.C., Martínez, A.M. and Eguía, V.M. (2019). Analysis of the influence of the variables of the Fused Deposition Modeling (FDM) process on the mechanical properties of a carbon fiber-reinforced polyamide. Procedia Manufacturing, 41, pp.731–738. doi:https://doi.org/10.1016/j.promfg.2019.09.064.

[9] Ajay Kumar, M., Khan, M.S. and Mishra, S.B. (2020). Effect of machine parameters on strength and hardness of FDM printed carbon fiber reinforced PETG thermoplastics. Materials Today: Proceedings. doi:https://doi.org/10.1016/j.matpr.2020.01.291.

[10] Lee, C.H., Padzil, F.N.B.M., Lee, S.H., Ainun, Z.M.A. and Abdullah, L.C. (2021). Potential for Natural Fiber Reinforcement in PLA Polymer Filaments for Fused Deposition Modeling (FDM) Additive Manufacturing: A Review. Polymers, 13(9), p.1407. doi:https://doi.org/10.3390/polym13091407.

[11] Durga Prasada Rao, V., Rajiv, P. and Navya Geethika, V. (2019). Effect of fused deposition modelling (FDM) process parameters on tensile strength of carbon fibre PLA. Materials Today: Proceedings. doi:https://doi.org/10.1016/j.matpr.2019.06.009.

[12] Maqsood, N. and Rimašauskas, M. (2021). Characterization of carbon fiber reinforced PLA composites manufactured by fused deposition modeling. Composites Part C: Open Access, 4, p.100112. doi:https://doi.org/10.1016/j.jcomc.2021.100112.

[13] Karimi, A., Davood Rahmatabadi and Mostafa Baghani (2024). Various FDM Mechanisms Used in the Fabrication of Continuous-Fiber Reinforced Composites: A Review. Polymers, 16(6),pp.831–831. doi: https://doi.org/10.3390/polym16060831.

[14] Hu, Y., Ladani, R.B., Brandt, M., Li, Y. and Mouritz, A.P. (2021). Carbon fibre damage during 3D printing of polymer matrix laminates using the FDM process. Materials

& Design, 205, p.109679. doi:https://doi.org/10.1016/j.matdes.2021.109679.

[15] Selvam, A., Mayilswamy, S., Whenish, R., Velu, R. and Subramanian, B. (2020). Preparation and Evaluation of the Tensile Characteristics of Carbon Fiber Rod Reinforced 3D Printed Thermoplastic Composites. Journal of Composites Science, 5(1),p.8. doi:https://doi.org/10.3390/jcs5010008.

[16] Ning, F., Cong, W., Qiu, J., Wei, J. and Wang, S. (2015). Additive manufacturing of carbon fiber reinforced thermoplastic composites using fused deposition modeling. Composites Part B: Engineering, 80, pp.369–378. doi:https://doi.org/10.1016/j.compositesb.2015.06.013.

[17] Uşun, A. and Gümrük, R. (2021). The mechanical performance of the 3D printed composites produced with continuous carbon fiber reinforced filaments obtained via melt impregnation. Additive Manufacturing, 46, p.102112. doi:https://doi.org/10.1016/j.addma.2021.102112.

[18] Mishra, P.K., Bandi Karthik and T. Jagadesh (2023). Finite Element Modelling and Experimental Investigation of Tensile, Flexural, and Impact Behaviour of 3D-Printed Polyamide. Journal of The Institution of Engineers (India) Series D, 105(1), pp.275–283. doi:https://doi.org/10.1007/s40033-023-00477-8.

[19] Mishra, P.K., kumar, D.S., T Jagadesh and Shukla, K. (2023). Experimental investigation into flexural and impact behaviour of 3D printed PETG short carbon fibre composite under solar light irradiation. Proceedings of the Institution of Mechanical Engineers Part C Journal of Mechanical Engineering Science, 237(16), pp.3597–3607. doi:https://doi.org/10.1177/09544062211149923.

[20] Valvez, S., Santos, P., Parente, J.M., Silva, M.P. and Reis, P.N.B. (2020). 3D printed continuous carbon fiber reinforced PLA composites: A short review. Procedia Structural Integrity, 25, pp.394–399. doi:https://doi.org/10.1016/j.prostr.2020.04.056.

[21] V. C. Gavali, P. R. Kubade, H. B. Kulkarni, and V. C. Gavali (2020) Mechanical and Thermo-mechanical Properties of Carbon fiber Reinforced Thermoplastic Composite Fabricated Using Fused Deposition Modeling Method. Materials Today: Proceedings 22 (2020) 1786–1795

[22] Bilkar, D., Keshavamurthy, R. and Tambrallimath, V. (2020). Influence of carbon nanofiber reinforcement on mechanical properties of polymer composites developed by FDM. Materials Today: Proceedings. doi:https://doi.org/10.1016/j.matpr.2020.09.707.

[23] Choudhari, D.S. and Kakhandki, V.J. (2021). Comprehensive study and analysis of mechanical properties of chopped carbon fibre reinforced nylon 66 composite materials. Materials Today: Proceedings, 44, pp.4596–4601. doi:https://doi.org/10.1016/j.matpr.2020.10.828.

[24] Z. Zhang and I. Fidan (2019), Failure Detection of Fused Filament Fabrication via Deep Learning in Solid Freedom Fabrication Symposium - An Additive Manufacturing Conference, Cookeville, pp. 2156–2164.

[25] Rajendran Royan, N.R., Leong, J.S., Chan, W.N., Tan, J.R. and Shamsuddin, Z.S.B. (2021). Current State and Challenges of Natural Fibre-Reinforced Polymer Composites as Feeder in FDM-Based 3D Printing. Polymers, 13(14), p.2289. doi:https://doi.org/10.3390/polym13142289.

[26] Alarifi, I.M. (2022). A performance evaluation study of 3d printed nylon/glass fiber and nylon/carbon fiber composite materials. Journal of Materials Research and Technology, 21, pp.884–892. doi:https://doi.org/10.1016/j.jmrt.2022.09.085.

[27] Fidan, I., Imeri, A., Gupta, A., Hasanov, S., Nasirov, A., Elliott, A., Alifui-Segbaya, F. and Nanami, N. (2019). The trends and challenges of fiber reinforced additive manufacturing. The International Journal of Advanced Manufacturing Technology, [online] 102(5-8), pp.1801–1818. doi:https://doi.org/10.1007/s00170-018-03269-7.

[28] Mohammadizadeh, M., Gupta, A. and Fidan, I. (2021). Mechanical benchmarking of additively manufactured continuous and short carbon fiber reinforced nylon. Journal of Composite Materials, p.002199832110200. doi:https://doi.org/10.1177/00219983211020070.

[29] Orkhan Huseynov, Seymur Hasanov and Ismail Fidan (2023). Influence of the matrix material on the thermal properties of the short carbon fiber reinforced polymer composites manufactured by material extrusion. Journal of Manufacturing Processes, 92, pp.521–533. doi:https://doi.org/10.1016/j.jmapro.2023.02.055.

[30] Kumar Mishra, P. and T., J. (2024). Comparison study of Izod impact properties on 3D printed thermoplastic and thermoset carbon fiber composite at different infill density. Rapid Prototyping Journal. doi:https://doi.org/10.1108/rpj-01-2024-0003.

[31] Test Methods for Determining the Izod Pendulum Impact Resistance of Plastics. (n.d.). doi:https://doi.org/10.1520/d0256-10.

[32] Inernational Astm (2007). Standard Test Methods for Flexural Properties of Unreinforced and Reinforced Plastics and Electrical Insulating Materials.

[33] Test Method for Tensile Properties of Plastics. (n.d.). doi:https://doi.org/10.1520/d0638-22.

[34] Sharma, P., Vaid, H., Vajpeyi, R., Shubham, P., Agarwal, K.M. and Bhatia, D. (2022). Predicting the dimensional variation of geometries produced through FDM 3D printing employing supervised machine learning. Sensors International, 3, p.100194. doi:https://doi.org/10.1016/j.sintl.2022.100194.

[35] Giannakis, C. Koidis, P. Kyratsis (2019) Static and Fatigue Properties of 3d Printed Continuous Carbon Fiber Nylon Composites. International Journal of Modern Manufacturing Technologies, vol. XI, no. 3.

[36] Mohammadizadeh, M. and Fidan, I. (2021). Tensile Performance of 3D-Printed Continuous Fiber-Reinforced Nylon Composites. Journal of Manufacturing and Materials Processing, 5(3), p.68. doi:https://doi.org/10.3390/jmmp5030068.